Materials Science Forum *Online: 2005-09-15*
ISSN: 1662-9752, Vols. 495-497, pp 1553-1558
doi:10.4028/www.scientific.net/MSF.495-497.1553

Effects of Texture and Anisotropy on Intergranular Stress Development in Zirconium

E.C. Oliver[1, a], M.R. Daymond[2,b] and P.J. Withers[3,c]

[1]ISIS Neutron Scattering Facility, Rutherford Appleton Laboratory, Chilton, Didcot, OX11 0QX, UK

[2]Dept. of Mechanical and Materials Engineering, Queen's University, Ontario, K7L 3N6, Canada

[3]Manchester Materials Science Centre, Grosvenor St, Manchester, M1 7HS, UK

[a]e.c.oliver@rl.ac.uk, [b]daymond@me.queensu.ca, [c]p.j.withers@man.ac.uk

Keywords: Texture, anisotropy, zirconium, neutron diffraction, residual stress

Abstract. The influence of texture and anisotropy on the generation of intergranular stresses in clock-rolled zirconium is investigated using neutron diffraction and elastoplastic self-consistent modelling. Comparison between experimental data and model calculations indicates that the operation mainly of prismatic and basal slip explains the trends in intergranular stress evolution during in-plane tensile and through-thickness compressive deformation, whilst twinning plays a significant role during in-plane compression.

Introduction

The intergranular stresses which develop in polycrystalline alloys during plastic deformation are directly attributable to the effects of anisotropy at the single crystal level, and to the orientation distribution of crystallites comprising the polycrystal. Neutron diffraction has become established as a central technique for the investigation of these intergranular stresses [1-4]. In the study reported here, the method has been applied to investigate intergranular stress evolution during uniaxial deformation of textured zirconium. Alloys of zirconium are of considerable importance to the nuclear industry, and there has been considerable effort over a number of years to characterise the effects of texture on the mechanical behaviour of this material [4-7]. While there have been a few previous neutron studies for this purpose [4,7], the present contribution is novel in investigating how intergranular stresses develop when the material is subjected to different deformation senses and loading axes. By comparison with calculations using an elastoplastic self-consistent model, this provides valuable information concerning the deformation modes which are activated during straining.

Methods

The material investigated in this study was crystal-bar zirconium subjected to a series of clock rolling and vacuum annealing cycles. This produces a strong basal texture and approximate axisymmetry about the plate normal direction. Typical pole figures for the material processed via this route can be seen in references [6,7]. Tensile and compressive specimens of cross-sectional area ~25mm^2 were machined for room temperature uniaxial loading in in-plane compression (IPC) and tension (IPT) and through thickness compression (TTC). Time-of-flight neutron diffraction spectra were recorded in situ during loading using the ENGIN-X instrument, ISIS, UK. This instrument is a modern, dedicated engineering diffractometer, designed to optimise measurements of internal stresses. It has two banks of scintillator detectors centred at horizontal scattering angles of +/-90º to the incident beam. Spectra were recorded with scattering vectors aligned parallel and transversely to the applied uniaxial load. The acquisition of each full diffraction profile required a counting time of approximately 3 mins, during which interval the applied load was maintained at a constant level. Grain family elastic strains were extracted from the data by applying single peak fitting to monitor diffraction peak shifts. Macroscopic strain was measured using an extensometer.

Elastoplastic self-consistent model simulations were performed for comparison to the data using the model implementation described elsewhere [5]. The input parameters for the model are the single crystal elastic constants, critical resolved shear stresses and hardening parameters for the specified plastic deformation modes, and a discrete population of grain orientations representative of the material's texture. In this case, a representative population was achieved by fitting the observed axial and transverse diffraction spectra to a spherical harmonic texture representation in the GSAS structural analysis software package, exploiting the axisymmetry of the material. Grain orientations were then attributed weights to match this texture using the popLA texture analysis suite. The single crystal elastic constants were taken from the literature [8], and critical resolved shear stress and hardening components were varied in order to gain best agreement between the model calculations and the observed macroscopic and internal strain data. The objective was not to use the model as a predictive tool, but rather to assist in interpreting the internal strain data in terms of operative deformation modes.

Results and Discussion

Examples of diffraction spectra acquired prior to deformation in the plate normal and in-plane directions are shown in Fig. 1. The strong basal texture is evident from the absence of the $\{10\bar{1}0\}$ peak in the normal direction spectrum, and the almost complete absence of the {0002} reflection in the in-plane spectrum. The effect of the strong texture is clearly seen in the macroscopic stress-strain responses in the various tests, shown in Fig. 2. The yield stress is lowest for IPT deformation, whilst a similar but slightly harder response is observed for IPC deformation. In TTC deformation, large scale yielding requires a stress approximately 3 times as large. It has previously been established that this hard response is due to the fact that zirconium crystallites offer considerable resistance to compressive deformation parallel to the basal pole, due to the unavailability of "easy" deformation modes to accommodate such strain [6].

Neglecting the possibility of the presence of thermal residual stresses, one would expect the IPC and IPT flow curves to be the same if deformation is accommodated fully by slip plasticity, due to the inherent bi-directionality of slip. However, it was noted that the intensity of the in-plane {0002} reflection grew significantly during the early stages of IPC deformation, but not during IPT deformation. This points to the operation of $\{10\bar{1}2\} < \bar{1}011 >$ twinning during IPC straining, since the crystallite re-orientation caused by this mechanism would explain the rapid emergence of the {0002} peak. This twinning mode, which is known to operate in Zr [6], gives rise to elongation along the basal pole. Since the poles tend to lie transversely during in-plane straining, the mechanism would thus be favoured by compression along the in-plane direction. If the operation of twinning is indeed responsible for the harder IPC response, it appears that the emergence of twin boundaries has a significant hardening effect on the operative slip systems.

The elastic strains which develop axially and transversely relative to the tensile axis are plotted for selected grain families against applied stress in Fig. 3. Comparing the data for the IPT and IPC tests, significant differences are apparent, despite the fact that the macroscopic curves are so similar. For the IPT test, the axial strains developed in all families are similar (hence data is only shown for three families, to maintain clarity). The $\{10\bar{1}0\}$ and $\{11\bar{2}0\}$ families follow one another very closely, while the $\{10\bar{1}1\}$ develops a greater strain before inflecting back. In the IPC axial data, there is a greater separation between $\{10\bar{1}0\}/\{11\bar{2}0\}$ and $\{10\bar{1}1\}$. However, it is transversely to the tensile axis (along the plate normal direction) that the differences between IPC and IPT straining are most clearly seen. Along this direction, very large strain differences develop between families during IPT deformation, whereas all families develop similar Poisson strains in the IPC

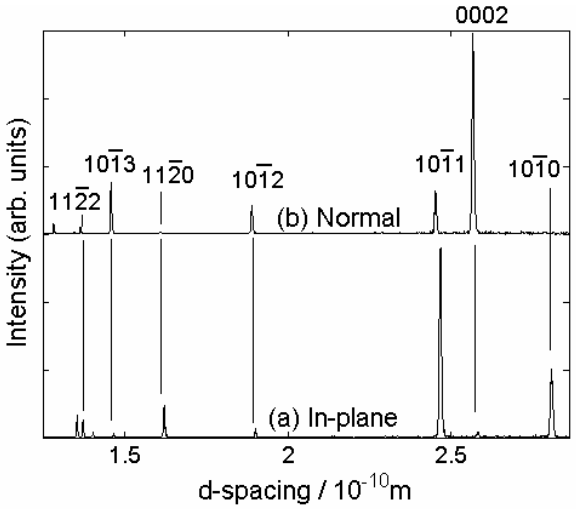

Fig. 1. Neutron diffraction spectra of clock-rolled zirconium prior to uniaxial deformation: (a) in-plane direction; (b) plate normal direction.

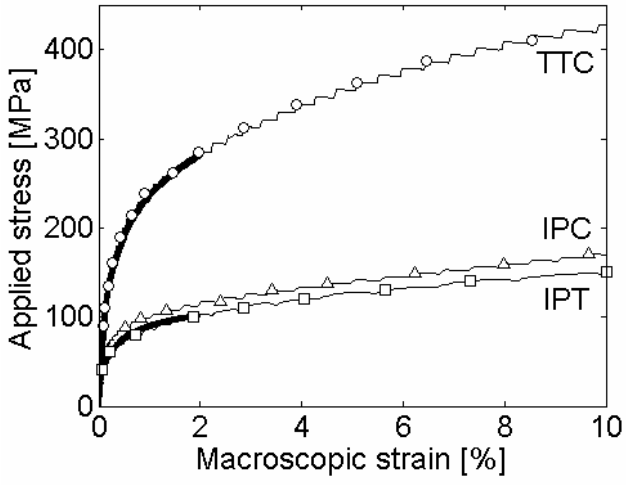

Fig. 2. Macroscopic stress-strain curves for in-plane tension (IPT), in-plane compression (IPC) and through-thickness compression (TTC). Thin lines joined by occasional datapoints represent data measured during in-situ neutron data acquisition; the bold lines for IPT and TTC correspond to curves calculated using the EPSC method.

test. This provides further evidence of an additional deformation mode available for IPC straining – namely, twinning. Also shown for the IPC test is the {0002} axial strain, which grows very rapidly. This strain corresponds to the initially small number of grains oriented with the basal pole parallel to the in-plane direction. Since these grains cannot easily accommodate compressive strain, a large misfit develops between them and their surroundings, explaining the rapid development of intergranular stress. As twinning progresses, the population of these grains increases. This provides a source of work hardening which may in part explain the difference between the IPC and IPT flow curves. There appears to be an inflection towards lower strain in the other grain families at approximately 130MPa, which may be due to load transfer towards the growing twin population.

Large intergranular strains are evident in the axial data for the TTC test. Generally, the families which bear the largest strains are those in which the basal poles lie closest the to compression axis, with {0002} developing the largest strain, for the same reason explained above. A strong correlation exists between this dataset and the transverse IPT dataset, since both correspond to the development of compressive strain along the plate normal direction.

EPSC Model Comparisons

The IPT and TTC datasets presented in Fig. 2 are now compared to EPSC model calculations. Due to the complexities introduced when twinning plays a significant role (due to slip/twinning interactions and evolving twin volume fraction), simulations of the IPC deformation are not presented here but will be considered in detail elsewhere.

Prismatic slip is accepted to be the primary slip mode in zirconium alloys. However, there is some debate as to whether basal slip also operates to a significant extent [4-6]. The simulations presented here adopt both modes, as well as <c+a> pyramidal slip, which is known to be much harder to activate but is required to accommodate basal pole compression. Twinning is not considered, since it is assumed that twinning deformation is insignificant in the IPT and TTC tests.

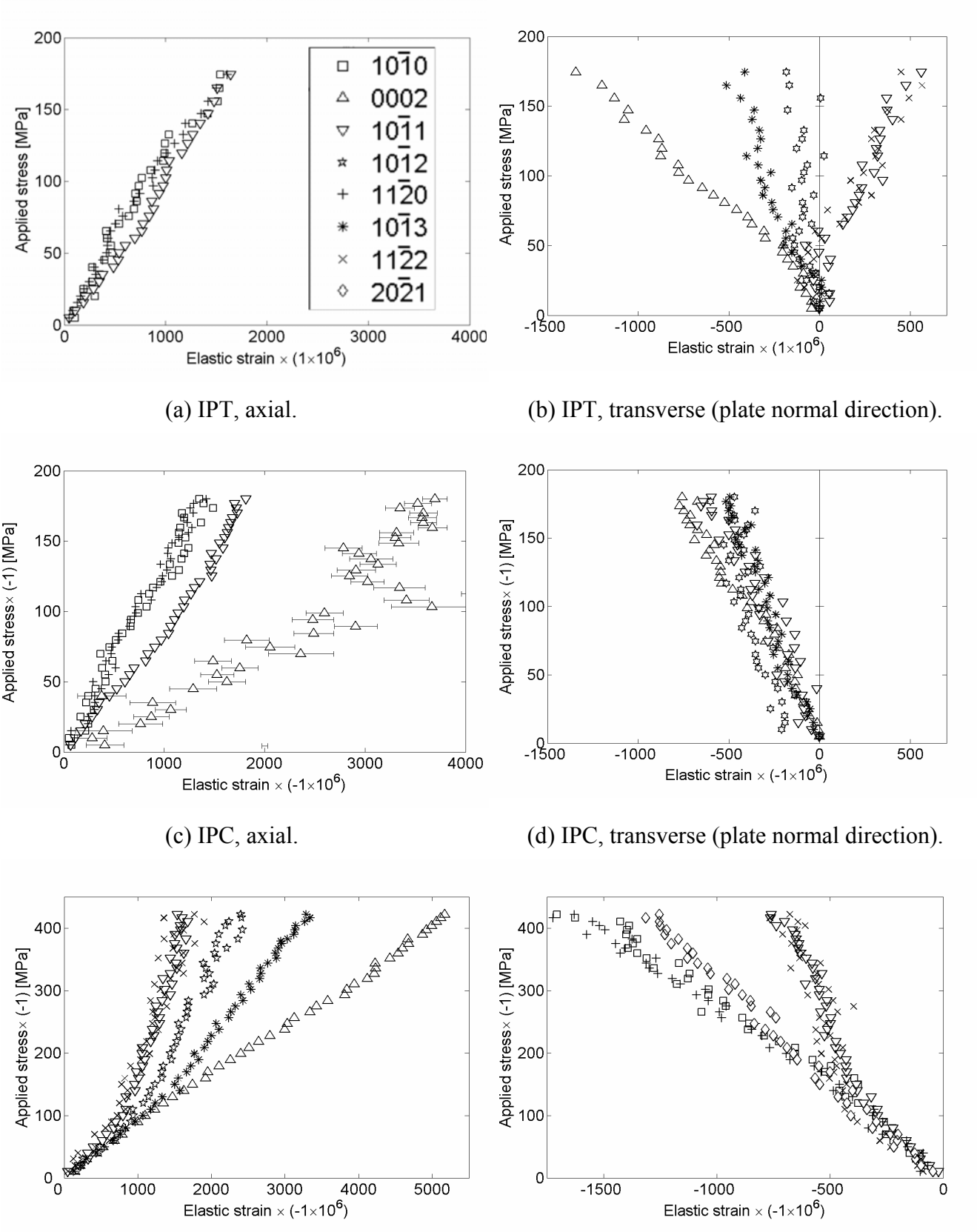

(a) IPT, axial.

(b) IPT, transverse (plate normal direction).

(c) IPC, axial.

(d) IPC, transverse (plate normal direction).

(e) TTC, axial.

(f) TTC, transverse.

Fig. 3. Lattice strains measured by neutron diffraction axially and transversely to uniaxially applied stress. In the plots corresponding to compressive tests, the x- and y- axes of the plots are multiplied by –1, for the purpose of comparison to the tensile loading data. The legend in (a) applies to all plots.

System s	τ_0 (MPa)	τ_1 (MPa)	θ_0 (MPa)	θ_1 (MPa)
Prismatic $\{10\bar{1}0\}<\bar{1}2\bar{1}0>$	10	1	2000	100
Basal $\{0001\}<11\bar{2}0>$	40	8	2000	100
Pyramidal $\{10\bar{1}1\}<\bar{1}\bar{1}23>$	240	270	3000	250

Table 1. Fitted yield and hardening parameters for EPSC simulations.

Due to its anisotropic thermal expansion coefficients, zirconium is known to develop significant thermal residual stresses. We do not expect large thermal stresses in this particular case, however. This is due to the strong alignment of basal poles around the plate normal direction coupled with the fact that the single crystal thermal expansion ellipsoid is axisymmetric about the basal pole. In the EPSC simulations, we therefore ignore the presence of thermal stresses prior to deformation. In addition, we assume isotropic hardening of slip systems. Since the EPSC model is a small strain formulation which does not incorporate grain rotation, the calculations are restricted to maximum macroscopic strain of 2%.

The EPSC implementation employs an extended Voce hardening law parameterized by:

$$\hat{\tau} = \tau_0 + \left(\tau_1 + \theta_1\Gamma\right)\left(1 - \exp - \left(\frac{\theta_0\Gamma}{\tau_1}\right)\right) . \qquad (1)$$

The parameters which produce the best agreement with both the macroscopic and internal strain data are given in Table 1. The critical resolved shear stress (τ_0) is lowest by far for prismatic slip, and very large for pyramidal slip. The calculated macroscopic flow curves corresponding to these parameters are shown as bold lines on Fig. 2. It can be seen that the large difference in yield stress between the IPT and TTC curves is well captured. The internal strain calculations are plotted with the corresponding experimental data in Fig. 4. The agreement is very good except in the case of the transverse IPT data. The trends are generally correct even in this case, and it has been shown that transverse strains are very sensitive to small variations in texture [10], so the numerical discrepancies may be partly due to the simplistic texture representation adopted.

Overall, the agreement is sufficiently good to instill confidence that the operative deformation modes in the simulations bear a close relation to those which operate in the real material. Two significant findings result from this. Firstly, the contribution from pyramidal slip is very small even in TTC deformation. The value of τ_0 is so high for this mode that the calculated intergranular strains are effectively explained by the operation of prismatic and basal slip only. Secondly, although prismatic slip is indeed the most active mode, basal slip is also important. Simulations without the incorporation of basal slip generally produce much poorer agreement with the experimental data. This is notable, since the influence of basal slip has previously been ignored in texture simulations [7]. It is basal slip which causes the axial IPT $\{10\bar{1}1\}$ response to inflect back towards the $\{10\bar{1}0\}$ and $\{11\bar{2}0\}$ responses. Since this inflection is less distinct in the IPC dataset, it may be speculated that the operation of twinning provides a greater barrier to basal slip than to prismatic slip.

Conclusion

This work has shown that large incompatibilities between grains develop during plastic deformation of zirconium, due largely to the difficulty in accommodating compressive strains parallel to the basal pole. The intergranular stresses which result have been explained using simple arguments and self-consistent calculations, enabling deductions to be made about the deformation modes which operate during straining.

Acknowledgements

The authors are extremely grateful to Dr Carlos Tomé and the Materials Science and Technology Department of Los Alamos National Laboratory for assistance and the provision of material and the EPSC code. This work was funded under EPSRC project GR/R07936.

References

[1] B. Clausen, T. Lorentzen, M. Bourke, M.R. Daymond: Mater. Sci. Eng. Vol. A259 (1999) 17.
[2] E.C. Oliver, M.R. Daymond, J. Quinta da Fonseca, P.J. Withers: J. Neut. Res. Vol. 12 (2004) 33
[3] E.C. Oliver, M.R. Daymond, P.J. Withers: Acta Mater. Vol. 52 (2004) 1937.
[4] J.W.L. Pang, T.M. Holden, P.A. Turner, T.E. Mason: Acta Mater. Vol. 47 (1999) 373.
[5] P.A. Turner, C.N. Tomé: Acta Metall. Vol. 42 (1994) 4043.
[6] C.N. Tomé, P.J. Maudlin, R.A. Lebensohn, G.C. Kaschner: Acta Mater. Vol. 49 (2001), p. 3085.
[7] P. Rangaswamy, M.A.M. Bourke, D.W. Brown, G.C. Kaschner, R.B. Rogge, M.G. Stout, C.N. Tomé: Metall. Mater. Trans. Vol 33A (2002), p. 757
[8] E.A. Brandes (ed.): Smithells Metals Reference Book 7th ed. (Butterworth-Heinemann 1998).

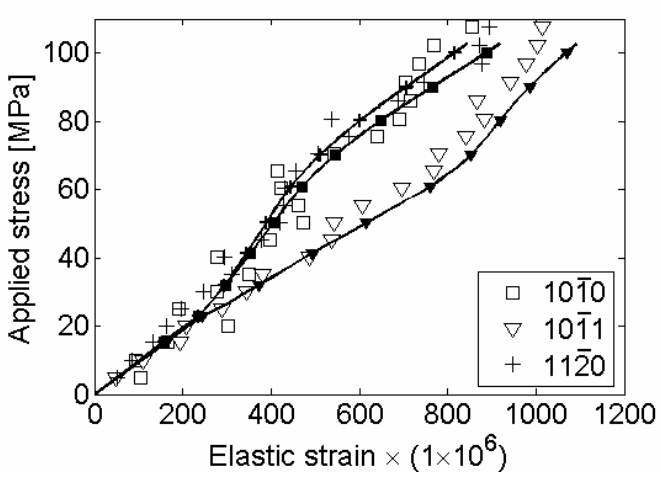

(a) IPT, axial.

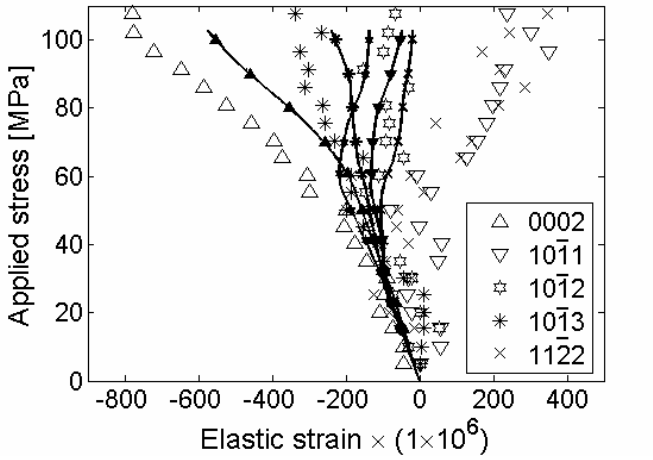

(b) IPT, transverse (plate normal direction).

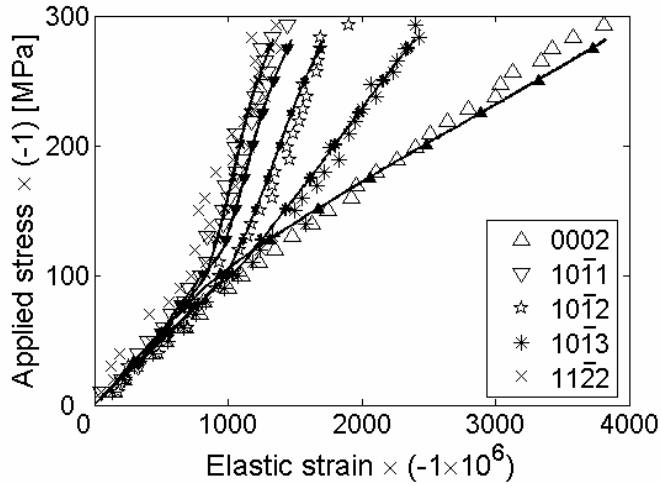

(c) TTC, axial.

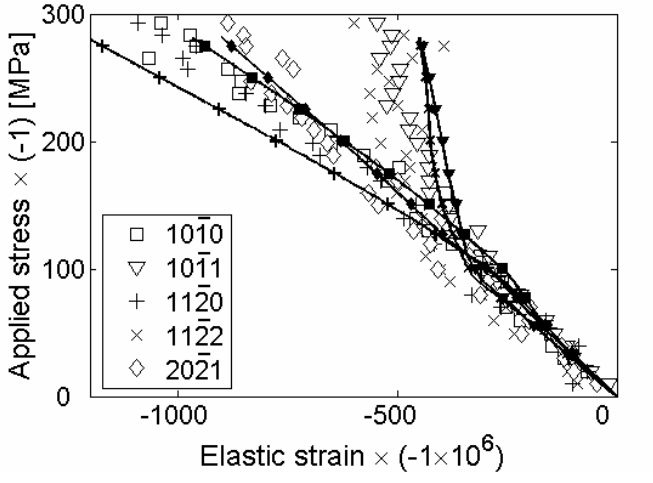

(d) TTC, transverse.

Fig. 4: EPSC-calculated lattice strains (lines+filled datapoints) and experimental data (unfilled datapoints) for the cases of in-plane tension (IPT) and through thickness compression (TTC).